Conditional *Pten* knockout in parvalbumin- or somatostatin-positive neurons sufficiently leads to autism-related behavioral phenotypes

Sangyep Shin, Shiyong Huang*

Program in Neuroscience, Hussman Institute for Autism, Baltimore, Maryland 21201, USA

*Correspondence:

Email: shuang@hussmanautism

Address: 801 West Baltimore Street, Suite 301, Baltimore, Maryland 21201, USA

ABSTRACT

Disrupted interneurons have been extensively described in brain tissues from individuals with autism spectrum disorder (ASD) and animal models for ASD. However, the contribution of aberrant interneurons to autism-related behavioral phenotypes is not well understood. We examined ASD-related behaviors in mice with conditional *Pten* knockout in parvalbumin (PV)-expressing and somatostatin (Sst)-expressing neurons, two prominent subtypes of inhibitory neurons. We found that mice with deletion of *Pten* in either PV-neurons or Sst-neurons displayed social deficits, repetitive behaviors and impaired motor coordination/learning. In addition, mice with one copy of *Pten* deletion in PV-neurons exhibited hyperlocomotion in novel open fields. We also examined anxiety behaviors and found that mice with *Pten* deletion in Sst-neurons displayed anxiety-like behaviors, while mice with *Pten* deletion in PV-neurons exhibited anxiolytic-like behaviors. These behavioral assessments demonstrate that *Pten* knockout in the subtype of inhibitory neurons sufficiently gives rise to ASD-core behaviors, providing evidence that both PV- and Sst-neurons may play a critical role in ASD symptoms.

Keywords: Autism; Social deficits; Repetitive behaviors; Mouse model; *Pten*; Motor deficits

1. INTRODUCTION

Inhibitory interneurons are highly impacted in autism spectrum disorder (ASD) (Hussman, 2001; Marin, 2012; Rapanelli et al., 2017a), a neurodevelopmental condition characterized by symptoms of difficulty in communication, deficits in social interaction, and the presence of restricted/repetitive behaviors (Association, 2013). Soma-targeting parvalbumin (PV)-expressing neurons (PV-neurons) and dendritic-targeting somatostatin (Sst)-expressing neurons (Sst-neurons) are two prominent subtypes of inhibitory neurons in the cortex (Rudy et al., 2011). Studies of postmortem human brain tissues have demonstrated aberrant interneurons, mainly PV-neurons, in the brains of individuals with autism (Ariza et al., 2018; Hashemi et al., 2017; Soghomonian et al., 2017; Zikopoulos and Barbas, 2013). Disrupted interneurons have also been extensively reported in animal models for autism (Bridi et al., 2017; Lauber et al., 2018; Sohal and Rubenstein, 2019). However, the contribution of each subtype of inhibitory neurons to autism symptoms is largely unknown. Thus, evaluating the role of PV-neurons and Sst-neurons in autism behaviors is crucial for the development of treatments.

The autism-risk gene, phosphatase and tensin homolog on chromosome ten (*PTEN*), originally identified as a tumor suppressor gene, negatively regulates cell proliferation and growth by downregulating the phosphatidylinositol 3-kinase/AKT/mammalian target of rapamycin (PI3K/AKT/mTOR) pathway (Barker and Houlston, 2003; Gregorian et al., 2009; Maehama and Dixon, 1998; Stiles et al., 2004). *PTEN* germline mutations have been identified in individuals with ASD (Buxbaum et al., 2007; Goffin et al., 2001), and may account for up to 12% of ASD cases (Hobert et al., 2014; McBride et al., 2010; Varga et al., 2009). *Pten* is widely expressed in both glutamatergic and GABAergic neurons during development and adulthood (Ljungberg et al., 2009; Vogt et al., 2015). Since deletion of *Pten* is embryonically lethal, mice

with brain-region-specific *Pten* knockout or *Pten* haploinsufficiency have been investigated (Garcia-Junco-Clemente et al., 2013). These transgenic mice exhibited autism-related behaviors, including deficits in social interaction, repetitive behaviors, hyperlocomotion, and anxiety-like behaviors (Clipperton-Allen and Page, 2014; Clipperton-Allen and Page, 2015; Cupolillo et al., 2016; Kwon et al., 2006; Lugo et al., 2014; Napoli et al., 2012; Page et al., 2009). However, whether conditional knockout of *Pten* in subtypes of interneurons causes autism-behavioral phenotypes remains elusive.

We used the Cre/loxp recombination system to generate mice with *Pten* knockout in PV-neurons or Sst-neurons, and conducted a battery of behavioral tests to examine autism-related behavioral phenotypes in these mice. We found that conditional knockout *Pten* in PV-neurons or Sst-neurons is sufficient to result in autism-core symptoms, including social deficits and repetitive behaviors. We also showed that *Pten* in PV-neurons and Sst-neurons is crucial for motor coordination and learning. Finally, deletion of *Pten* in PV-neurons induces hyperlocomotion and anxiolytic-like behaviors whereas deletion of *Pten* in Sst-neurons causes anxiety-like behaviors. Collectively, *Pten* mutation in PV-neurons and Sst-neurons results in autism-related behavioral phenotypes.

2. RESULTS

2.1. Deletion of Pten in PV-neurons or Sst-neurons leads to social deficits

First, we examined the effect of conditional *Pten* knockout in parvalbumin-expressing neurons (PV-neurons) on social behaviors. We specifically deleted *Pten* in PV-neurons by crossing PV-Cre mice with $\text{Pten}^{\text{flox}}$ mice to generate PV-$\text{Cre}^{+/+}$/$\text{Pten}^{\text{fl/+}}$ mice (See Methods for details). Using these mice as breeders, we obtained offspring littermates with three genotypes, PV-$\text{Cre}^{+/+}$/$\textit{Pten}^{+/+}$ (PV-Pten-WT), PV-$\text{Cre}^{+/+}$/$\textit{Pten}^{\text{fl/+}}$ (PV-Pten-Het), and PV-$\text{Cre}^{+/+}$/$\textit{Pten}^{\text{fl/fl}}$ (PV-Pten-KO). These

three types of mice all have homozygous Cre but different copy of *Pten* in PV-neurons. Sociability test and social novelty test were performed in these mice using modified three-chamber social tests (Figure 1A). As shown in figure 1B, single or two copies of *Pten* deletion in PV-neurons did not change the social approach behaviors. All three types of PV-Pten mice spent more time with social partners than with objects in the sociability test. The preference index was not different among the three groups of PV-Pten mice (Figure 1B). In contrast, knockdown or knockout of *Pten* in PV-neurons impaired the social novelty preference. In social novelty test, only PV-Pten-WT mice spent more time interacting with novel social partners (Figure 1C). The preference index for social novelty decreased in PV-Pten-Het and PV-Pten-KO mice compared to that in PV-Pten-WT mice (Figure 1C).

Next, we evaluated the effect of conditional *Pten* knockout in somatostatin-expressing interneurons (Sst-neurons) on social behaviors. Using the same breeding strategy for PV-Pten mice, we obtained Sst-Pten littermates with three genotypes, Sst-Cre$^{+/+}$/*Pten*$^{+/+}$ (Sst-Pten-WT), Sst-Cre$^{+/+}$/*Pten*$^{fl/+}$ (Sst-Pten-Het), and Sst-Cre$^{+/+}$/*Pten*$^{fl/fl}$ (Sst-Pten-KO). We found that both Sst-*Pten*-WT and -KO but not Het- mice spent more time in the interaction areas for social partners in the sociability test (Figure 1D). This result was also confirmed by the preference index for sociability which was significantly lower in Sst-Pten-Het mice (Figure 1D). Similarly, in the social novelty test, both Sst-Pten-WT and -KO but not -Het mice spent more time in the interaction zones for novel social partners, but the duration difference between the interactions with familiar and novel social partners in Sst-Pten-KO mice was small (Figure 1E). Consistently, the preference indexes for social novelty was reduced in both Sst-Pten-Het and -KO mice (Figure 1E). Thus, Sst-Pten-Het mice displayed deficits in both sociability and social novelty preference,

and Sst-Pten-KO mice exhibited impairment in social novelty behavior. Collectively, elimination of Pten in either PV-neurons or Sst-neurons resulted in reduced social behaviors in mice.

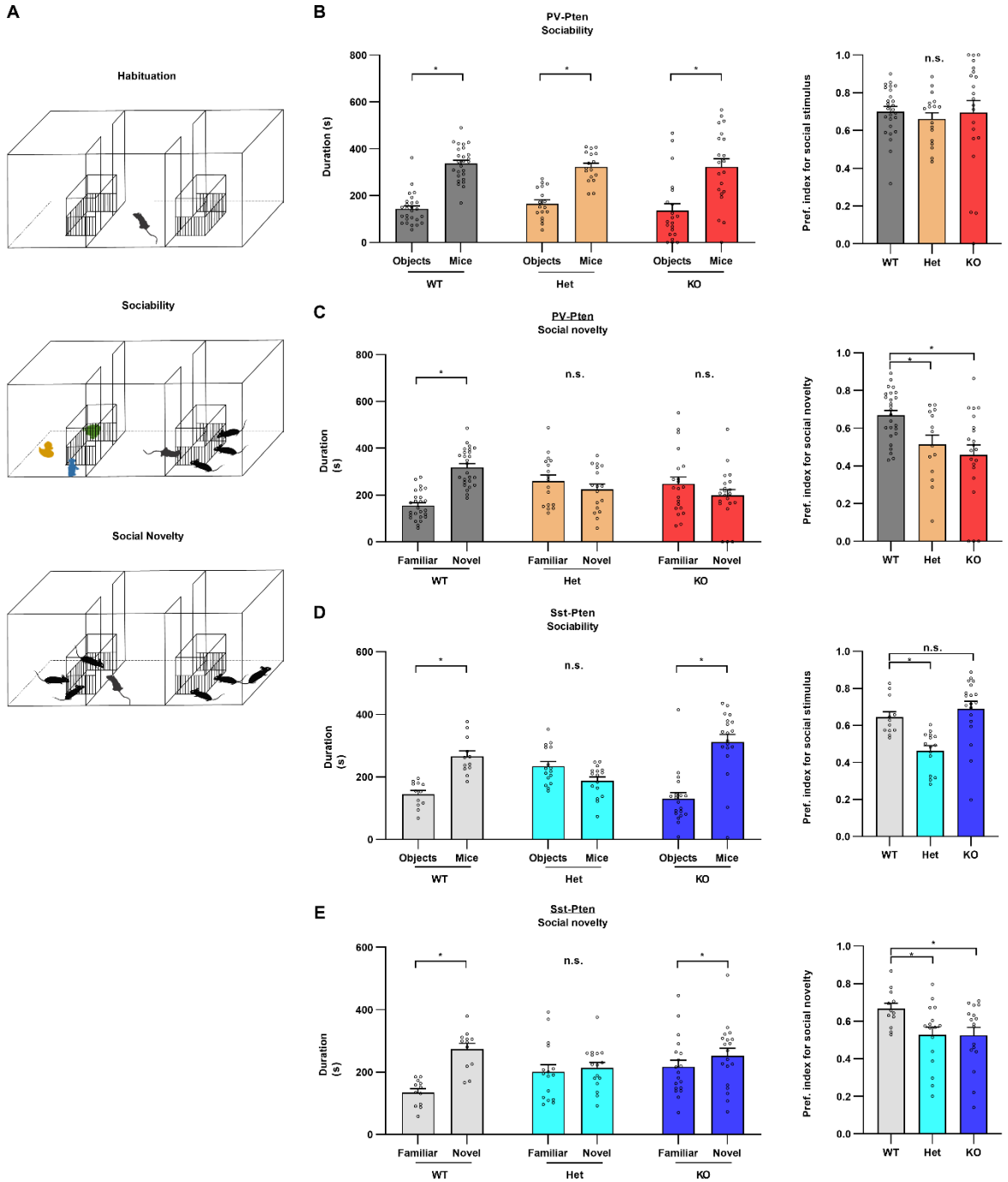

Figure 1. PV-Pten-KO and Sst-Pten-KO mice displayed social deficits in the modified three-chamber social test. (A) Schematic diagrams of the modified three-chamber social test. (**B**) Three genotypes of PV-Pten mice showed significant difference in the sociability test between objects and mice (social partners) (WT: n = 26, $t_{(50)}$ = 9.94, $p < 0.001$; Het: n = 17, $t_{(32)}$ = 6.924, $p < 0.001$; KO: n = 21, $t_{(40)}$ = 4.078, $p < 0.001$; Paired *t*-test). There is no significant difference in preference index for social stimulus among three genotypes of PV-Pten mice (WT: n = 26,

Het: n = 17, KO: n = 21; $F_{(2,61)}$ = 0.213, p = 0.809, ANOVA). (**C**) Only PV-Pten-WT mice displayed significant difference between familiar and novel mice in the social novelty test (WT: n = 26, $t_{(50)}$ = 6.562, p < 0.001; Het: n = 17, $t_{(32)}$ = 1.375, p = 0.179; KO: n = 21, $t_{(40)}$ = 4.078, p = 0.204; Paired t-test). The preference index for social novelty significantly reduced in PV-Pten-Het and PV-Pten-KO mice compared with PV-Pten-WT mice (WT: n = 26, Het: n = 17, KO: n = 21; $F_{(2,61)}$ = 7.402, p = 0.001, ANOVA; Het vs. WT: p = 0.044; KO vs. WT: p = 0.01; Tukey's post hoc test). (**D**) Sst-Pten-Het mice showed deficits in the sociability test (WT: n = 11, $t_{(20)}$ = 2.680, p = 0.016; Het: n = 12, $t_{(22)}$ = 0.651, p = 0.521; KO: n = 17, $t_{(32)}$ = 5.306, p < 0.001; Paired t-test). The preference index for social stimulus significantly reduced in Sst-Pten-Het but not Sst-Pten-KO mice (WT: n = 11, Het: n = 12, KO: n = 17; $F_{(2,37)}$ = 7.451, p = 0.002, ANOVA; Het vs. WT: p = 0.036; KO vs. WT: p = 0.774; Tukey's post hoc test). (**E**) Sst-Pten-Het and Sst-Pten-KO mice displayed deficits in the social novelty test (WT: n = 11, $t_{(20)}$ = 5.130 , p < 0.001 ; Het: n = 12, $t_{(22)}$ = 2.037, p = 0.053; KO: n = 17, $t_{(32)}$ = 2.204, p = 0.034; Paired t-test). The preference index for social novelty significantly reduced in Sst-Pten-Het and Sst-Pten-KO mice (WT: n = 11; Het: n = 12; KO: n = 17; $F_{(2,37)}$ = 4.510, p = 0.018, ANOVA; Het vs. WT: p = 0.039; KO vs. WT: p = 0.024; Tukey's post hoc test). The preference index was calculated as described in the methods. Data are represented as mean ± SEM. *: significant; n.s.: not significant.

2.2. Deficits of locomotion and motor coordination and increased repetitive behaviors in PV-Pten and Sst-Pten mice

We then examined the contribution of *Pten* mutations in interneurons to deficits in locomotive behaviors. 30-min open field tests were performed in PV-Pten mice (Figure 2A). PV-Pten-Het but not -KO mice traveled significantly longer distances compared to PV-Pten-WT (Figure 2B). When examined in 5-min intervals, the distance moved in PV-Pten-WT and-Het mice declined slightly over the 30-min testing period, and PV-Pten-Het consistently traveled longer distances in each interval. PV-Pten-KO mice maintained the same rate of activity over the 30-min testing time (p = 0.903, Pearson correlation test), but no statistical difference compared to PV-Pten-WT mice. Thus, PV-Pten-Het mice exhibited elevated locomotive activity (Figure 2C). The locomotive activity in Sst-Pten mice was not different among genotypes (Figure 2D), and was confirmed by measurements across 5-min intervals (Figure 2E).

We also examined self-grooming during the open field test for repetitive behaviors. PV-Pten-KO mice exhibited an increase of grooming bouts (Figure 3A) and spent more time in self-grooming in the open field (Figure 3B). Similarly, the number of grooming bouts and total time of self-grooming were increased in Sst-Pten-KO mice (Figure 3C and 3D). These data suggest

that deletion of *Pten* in PV-neurons or Sst-neurons induces repetitive behaviors, a core-domain of autism behaviors.

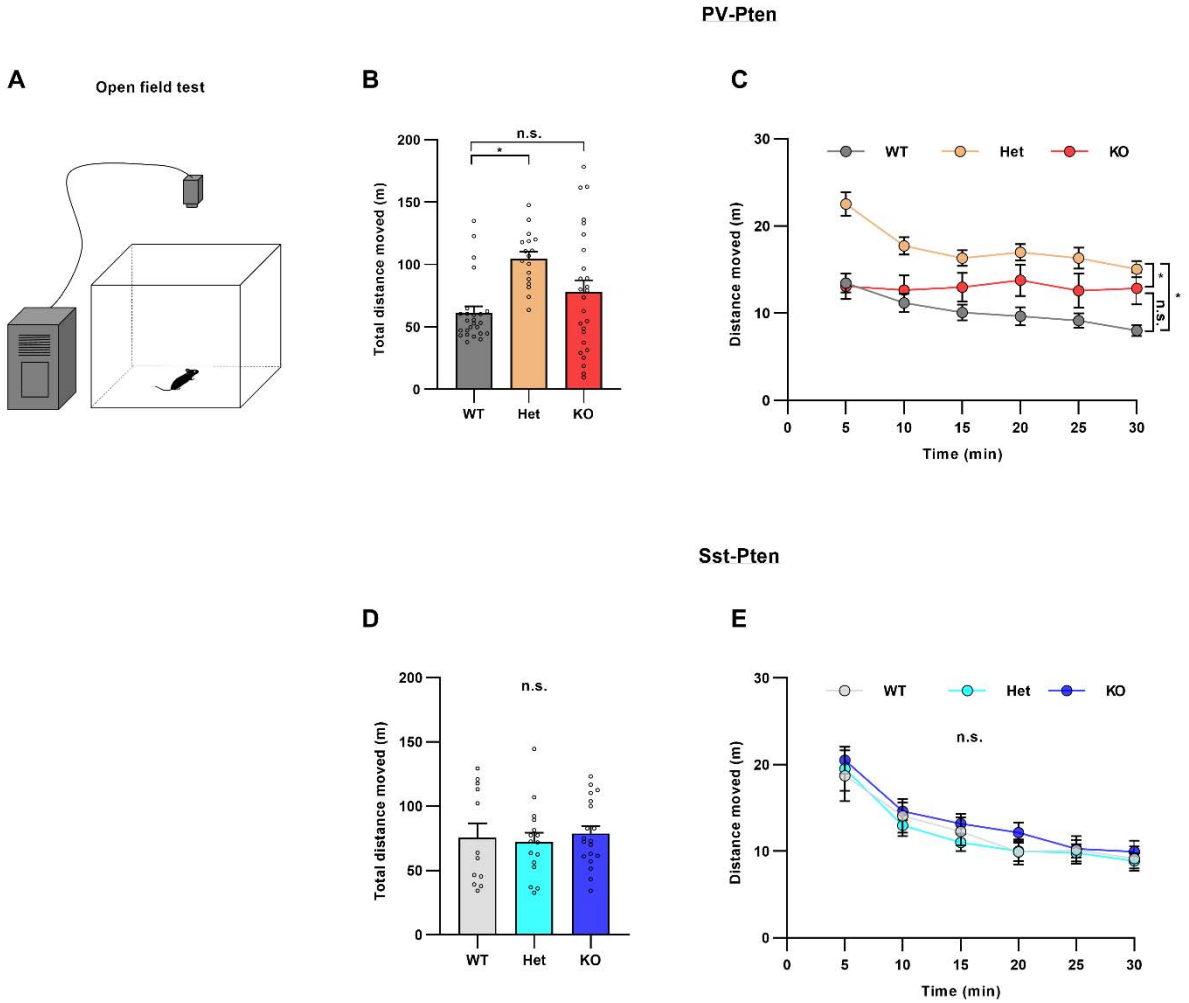

Figure 2. PV-Pten-Het exhibited hyperlocomotion in the open field test. (**A**) The schematic diagram of the open field test. (**B**) PV-Pten-Het mice traveled a longer distance than PV-Pten-WT during the 30-min test (WT: n = 25; Het: n = 17; KO; n = 26; $F_{(2,65)}$ = 7.244, p = 0.001, ANOVA. Het vs. WT: p < 0.001; KO vs. WT, p = 0.285; Tukey's post hoc test). (**C**) When total distance of PV-Pten mice was analyzed in 5-min time bin. PV-Pten-Het mice displayed hyperlocomotion (Het vs. WT, p < 0.001; KO vs. WT: p = 0.236; rmANOVA). (**D-E**) There is no significant difference in total distance moved (D) (WT: n = 12, Het: n = 16, KO: n = 19; $F_{(2,44)}$ = 0.313, p = 0.733, ANOVA) or distance moved in 5-min time bin (E) in Sst-Pten mice (p = 0.700, rmANOVA). Data are represented as mean ± SEM. *: significant; n.s.: not significant.

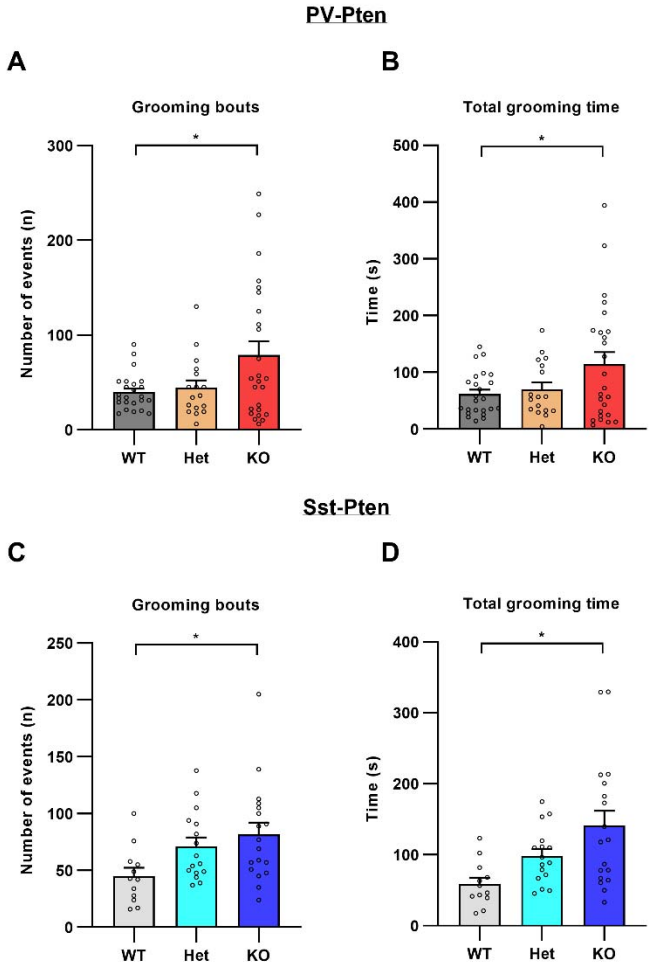

Figure 3. Increased self-grooming in PV-Pten-KO and Sst-Pten mice. (**A**) The number of self-grooming bouts increased in PV-Pten-KO mice (WT: n = 24; Het: n = 17; KO: n = 25; $F_{(2,63)}$ = 4.758, p = 0.012, ANOVA; KO vs. WT: p = 0.015; Tukey's post hoc test). (**B**) The total time of self-grooming increased in PV-Pten-KO mice (WT: n = 24; Het: n = 17; KO: n = 25; $F_{(2,63)}$ =3.635, p = 0.032, ANOVA; KO vs. WT: p = 0.036; Tukey's post hoc test). (**C**) The number of self-grooming bouts increased in Sst-Pten-KO mice (WT: n = 12; Het: n = 16; KO: n = 18; $F_{(2,43)}$ = 4.025, p = 0.025, ANOVA; KO vs. WT: p = 0.02; Tukey's post hoc test). (**D**) The total time of self-grooming increased in Sst-Pten-KO mice (WT: n = 12; Het: n = 16; KO: n = 18; $F_{(2,43)}$ = 6.249, p = 0.004, ANOVA; KO vs. WT: p = 0.003; Tukey's post hoc test). Data are represented as mean ± SEM. *: statistically significant.

We further evaluated the motor coordination/learning in PV-Pten mice using the rotarod test (Figure 4A). The latency to fall was significantly reduced in PV-Pten-Het mice over the 6-trial training (Figure 4B). Motor coordination was also severely impaired in PV-Pten-KO mice. They were barely able to stay on the stationary rotarod (Figure 4B). We analyzed the learning

index (ratio of latency to fall between the 6th trial and the 1st trial) and found that knockout of *Pten* in PV-neurons impaired motor learning in the rotarod test (Figure 4C). Similarly, knockout of *Pten* in Sst-neurons impaired rotarod performance and motor learning (Figure 4D and 4E). Collectively, knockdown or knockout of *Pten* in PV-neurons or Sst-neurons impairs motor coordination and learning.

We also conducted marble burying tests in PV-Pten and Sst-Pten mice (Figure 4F). PV-Pten-KO mice buried significantly fewer marbles than PV-Pten-WT mice (Figure 4G), but there was no difference in the marble burying task among the three genotypes of Sst-Pten mice (Figure 4H). Since the burying of marbles entails physical motor activity, reduced marble burying activity in PV-Pten-KO mice may be mainly resulted from impaired motor coordination in this type of mice (Figure 4B).

2.3. Anxiolytic-like behavior in PV-Pten mice and anxiety-like behavior in Sst-Pten mice

Finally, we examined anxiety-like behaviors in mice with Pten deletion in interneurons using elevated plus maze tests (Figure 5A) and open field tests (Figure 5B). In the elevated plus maze, PV-Pten-KO mice spent increased percentage of time in the open arms and decreased percentage of time in the closed arms, compared to PV-Pten-WT and PV-Pten-Het mice (Figure 5C and 5D). Similarly, in the open field test, PV-Pten-KO mice spent increased time in the center area (Figure 5E), and decreased time in the corner area of the open field compared to PV-Pten-WT mice (Figure 5F). In contrast, Sst-Pten-KO mice showed a reduced percentage of time in the open arms and an increased percentage of time in the closed arms (Figure 5G and 5H). We did not observe any difference of time spent in the center or corner areas among the three genotypes of Sst-Pten mice (Figure 5I and 5J). Thus, we concluded that *Pten* knockout in the PV-neurons

induces anxiolytic-like behavior while *Pten* knockout in the Sst-neurons evokes anxiety-like behavior.

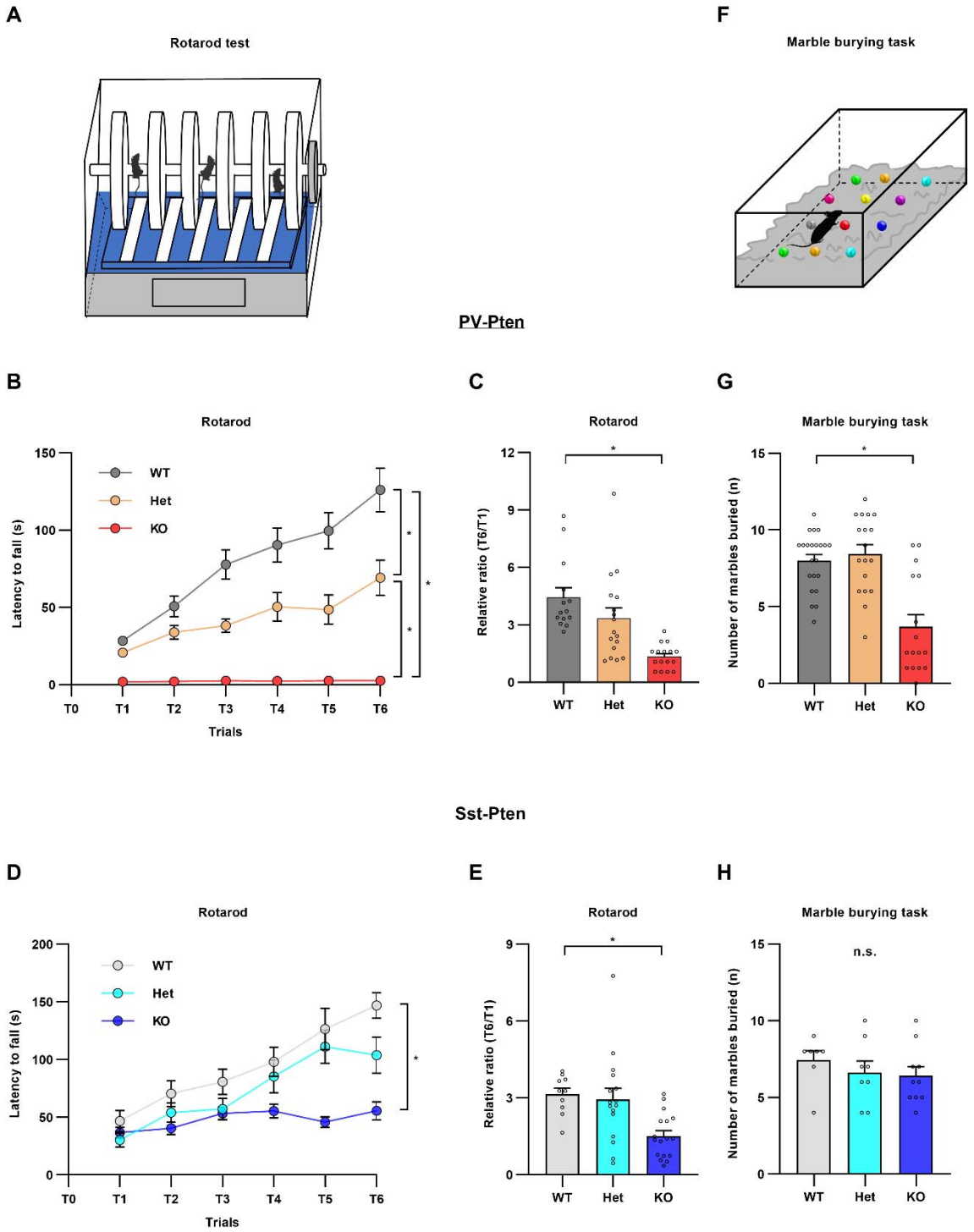

Figure 4. Impaired motor function in PV-Pten-KO and Sst-Pten-KO mice. (**A**) The schematic diagram of the rotarod test. (**B**) PV-Pten-Het and PV-Pten-KO mice showed a shorter latency to fall off the rotarod than PV-Pten-

WT over the 6-trials training (WT: n = 14, Het: n = 17, KO: n = 14; Het vs. WT: $p < 0.001$; KO vs. WT: $p < 0.001$; Het vs. KO: $p < 0.001$; rmANOVA). (**C**) The learning index (T6/T1) was significantly reduced in PV-Pten-KO mice ($F_{(2,44)} = 12.435$, $p < 0.001$, ANOVA; KO vs. WT: $p < 0.001$; Tukey's post hoc test). (**D**) Sst-Pten-KO mice showed a shorter latency to fall off the rotarod than Sst-Pten-WT mice over the 6-trials training (WT: n = 7, Het: n = 13, KO: n = 16; KO vs. WT: $p = 0.018$; rmANOVA). (**E**) The learning index (T6/T1) was significantly reduced in Sst-Pten-KO mice ($F_{(2,40)} = 7.372$, $p = 0.002$, ANOVA; KO vs. WT: $p = 0.007$; Tukey's post hoc test). (**F**) The schematic diagram of the marble burying test. (**G**) PV-Pten-KO mice buried significantly fewer marbles compared to PV-Pten-WT mice (WT: n = 22, Het: n = 18, KO: n = 16; $p < 0.001$, Kruskal-Wallis test; KO vs. WT, $p = 0.001$, Dunn's post hoc test). (**H**) There is no difference in the number of marbles buried among the three genotypes of Sst-Pten mice (WT: n = 7, Het: n = 8, KO: n = 10; $p = 0.406$, Kruskal-Wallis test). Data are represented as mean ± SEM. *: significant; n.s.: not significant.

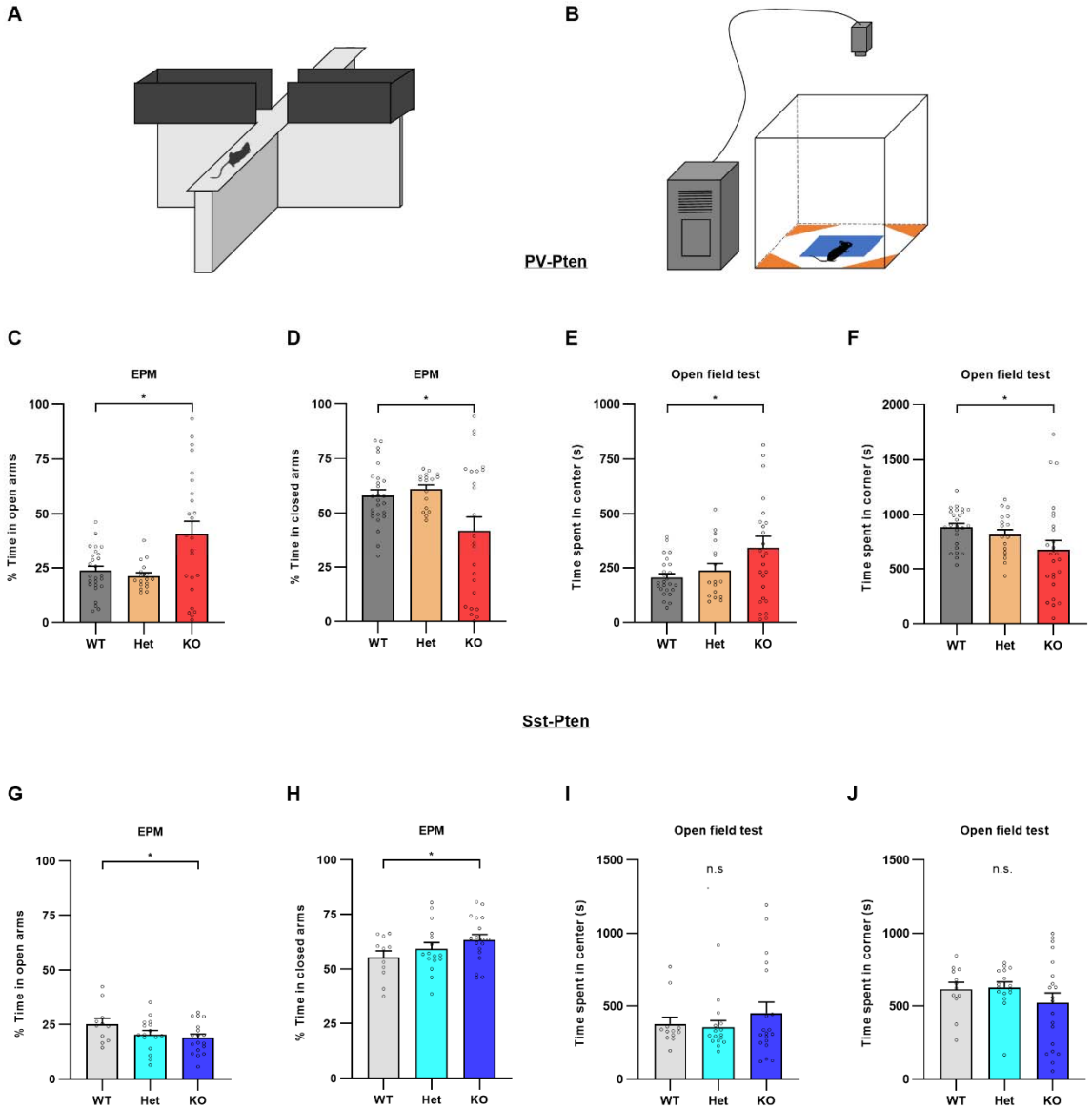

Figure 5. PV-Pten-KO mice showed anxiolytic behaviors while Sst-Pten-KO mice displayed anxiety-like behaviors, compared to their WT mice. (**A**) The schematic diagram of the elevated plus-maze test (EPM). (**B**) The schematic diagram of the center (blue) and corner area (orange) in the open field test. (**C**) PV-Pten-KO mice spend more percentage of time in the open arms compared to PV-Pten-WT and PV-Pten-Het mice (WT: n = 26, Het: n = 17, KO: n = 24; $F_{(2,64)} = 7.373$, $p = 0.001$, ANOVA; KO vs. WT, $p = 0.005$, Tukey's post hoc test). (**D**) PV-Pten-KO

mice spend less percentage of time in the closed arms compared to PV-Pten-WT and PV-Pten-Het mice ($F_{(2,64)}$ = 5.310, p = 0.007, ANOVA; KO vs. WT, p = 0.023, Tukey's post hoc test). (**E-F**) In the open field test, PV-Pten-KO mice spent more time in the center area (E) and less time in the corner area (F), compared to PV-Pten-WT mice (WT: n = 25, Het: n = 17, KO: n = 26; Center: p = 0.024, ANOVA; KO vs. WT, p = 0.023, Tukey's post hoc test; Corner: p = 0.016, Kruskal-Wallis test; KO vs. WT: p = 0.009, Dunn's post hoc test). (**G**) Sst-Pten-KO mice spend less percentage of time in the open arms compared to Sst-Pten-WT mice (WT: n = 11, Het: n = 16, KO: n = 17; $F_{(2,34)}$ = 3.984, p = 0.028, ANOVA; KO vs. WT: p = 0.026, Tukey's post hoc test). (**H**) Sst-Pten-KO spend more percentage of time in the closed arms compared to Sst-Pten-WT mice ($F_{(2,34)}$ = 3.596 , p = 0.038, ANOVA; KO vs. WT: p = 0.031, Tukey's post hoc test). (**I-J**) In the open field test, there is no difference in time spent in the center (I) or corner area (J) among the three genotypes of Sst-Pten mice (WT: n = 12, Het: n = 16, KO: n = 19; Center: p = 0.851; Corner: p = 0.502; Kruskal-Wallis test). Data are represented as mean ± SEM. *: significant; n.s.: not significant.

3. DISCUSSION

Our study revealed that conditional deletion of *Pten* in either PV-neurons or Sst-neurons results in autism-like core symptoms, including reduced social novelty preference and the presence of repetitive behaviors (self-grooming). In addition, conditional *Pten* knockout in PV-neurons causes differences in behaviors that are characteristic of symptoms often observed in autism, such as hyperactivity and impairment in motor coordination/learning. Similarly, conditional *Pten* knockout in Sst-neurons gives rise to disrupted motor coordination/learning. Interestingly, PV-Pten-KO mice displayed anxiolytic-like behaviors, whereas Sst-Pten-KO mice showed anxiety-like behaviors. These findings provide the behavioral evidence that *Pten* mutation in PV-neurons or Sst-neurons sufficiently induces ASD-related behaviors.

Mice with deletion of several other genes (*Shank2*, *mGluR5* and *Lom4*) in PV-neurons exhibit autism-related behaviors of varying severity (Barnes et al., 2015; Lee et al., 2018a; Zhang et al., 2020), supporting that the function of PV-neurons is an important determinant of autism behaviors. Autism-relevant behavioral phenotypes are also reported in mice with conditional *MeCP2* (Rett syndrome) or *Scn1a* (Dravet syndrome) knockout in PV-neurons but not Sst-neurons (Ito-Ishida et al., 2015; Tatsukawa et al., 2018). In our results, conditional knockout of

Pten in either PV- or Sst-neurons resulted in autism-like core behaviors, further suggesting that *Pten* plays an important role in the function of both subtypes of interneurons.

Multiple brain regions may be involved in the social deficits observed in PV-Pten-KO and Sst-Pten-KO mice (Modi and Sahin, 2019). The prefrontal cortex (PFC) is one such brain structure that is well established for social behaviors (Scheggia et al., 2020). PV-neurons and Sst-neurons in mPFC specifically respond to social stimuli (Selimbeyoglu et al., 2017; Sun et al., 2020). This social-evoked response in PV-neurons is diminished in mice with global deletion of the autism-risk gene *Cntnap2*, which display deficits in sociability (Selimbeyoglu et al., 2017). Consistently, optogenetic activation of PV-neurons in mPFC rescues deficits of sociability and social novelty in autism mouse models (Cao et al., 2018; Selimbeyoglu et al., 2017). However, evidence supporting a relationship between PV-neurons in mPFC and social deficits is not unequivocal (Murray et al., 2015).

The hippocampus is another brain region which is involved in social interaction, particular social memory, a process that is critical for preference for social novelty (Hitti and Siegelbaum, 2014; Okuyama et al., 2016). PV-neurons in the ventral hippocampus (vHipp) exhibited increased activity to novel social partners compared to familiar ones, and inactivation of PV-neurons but not Sst-neurons in vHipp disrupts social novelty (Deng et al., 2019). Conversely, knockdown Sst but not PV in vHipp disrupted social interaction (Perez et al., 2019).

The cerebellum was recently implicated in social behaviors (Carta et al., 2019; Tsai, 2016). PV and Sst are expressed in Purkinje cells (PC) of the cerebellum (Alcami and Marty, 2013; Asrican et al., 2013; Taniguchi et al., 2011). Abnormal PC function has been linked to social deficits in mice with conditional deletion of autism-risk genes in PCs (Peter et al., 2016; Reith et al., 2013; Stoodley et al., 2017; Tsai et al., 2012). However, conditional *Pten* knockout

in Purkinje cells results in autism-related behaviors, such as less time self-grooming and reduced sociability (Cupolillo et al., 2016), different phenotypes to those exhibited in PV-Pten-KO mice (increased self-grooming and deficits of social novelty). This discrepancy may be explained by the fact that Cre-recombinase activity in PV-Cre mice is not only present in Purkinje cells but also in cerebellar interneurons (Alcami and Marty, 2013; Zhang and Sudhof, 2016), indicating that cerebellar interneurons may contribute to behavioral phenotypes in PV-Pten-KO mice as well.

In addition, other brain regions, such as the amygdala (Felix-Ortiz and Tye, 2014; Hong et al., 2014), ventral tegmental area (VTA)-to nucleus accumbens (NAc) projection (Gunaydin et al., 2014), and the striatum (Lee et al., 2018b; Rapanelli et al., 2017b) all have been reported to be involved in social behaviors. Conditional *Pten* knockout in PV-neurons or Sst-neurons may impair inhibitory neural circuits in these brain areas and result in social deficits.

PV-Pten-KO mice and Sst-Pten-KO mice displayed impaired motor coordination/learning in accelerating rotarod tasks and increased repetitive behaviors (self-grooming) in open field tests. The cerebellum and striatum, two brain structures critical for motor coordination/learning and repetitive behaviors (Kayakabe et al., 2013; Wang et al., 2017; Whitehouse and Lewis, 2015), may account for these behavioral phenotypes. Additionally, *Pten* knockout in Purkinje cells results in impaired motor coordination/learning (Cupolillo et al., 2016), and inhibition of PCs in cerebellar right crus I results in repetitive behaviors (Stoodley et al., 2017). Moreover, *Pten* regulates striatal dopamine signaling (Diaz-Ruiz et al., 2009; Stavarache et al., 2015). All these lines of evidence indicate that motor deficits and repetitive behaviors in PV-Pten and Sst-Pten mice may result from the functional change of PV- and Sst-neurons in the cerebellum and/or striatum.

Our results showed that PV-Pten-KO mice exhibited anxiolytic-like behaviors while Sst-Pten-KO mice displayed anxiety-like behaviors. PV-neurons in the dentate gyrus of the hippocampus result in the anxiolytic behaviors (Zou et al., 2016). Disinhibition of PV-neurons by Sst-neurons (Pfeffer et al., 2013) may explain the differential effects of *Pten* knockout in these two subtypes of interneurons on anxiety-like behaviors.

At the synaptic level, conditional knockout *Pten* from GABAergic cortical interneurons increases the synaptic input onto interneurons (Barrows et al., 2017) and the inhibitory output onto glutamatergic neurons (Southwell et al., 2020; Vogt et al., 2015). Conversely, a single copy of Pten deletion from PV-neurons impairs the formation of perisomatic inhibition (Baohan et al., 2016). Though the underlying synaptic mechanisms in PV-Pten-KO and Sst-Pten-KO mice need further investigation, our results provide behavioral evidence that deletion of *Pten* in either subtype of inhibitory neurons elicits autism-related phenotypes, suggesting that a potential benefit from therapeutic strategies targeting either PV-neurons, Sst-neurons, or both subtypes, depending on specific alterations in behavioral phenotype.

4. MATERIAL AND METHODS

4.1. Animals

Pten$^{fl/+}$, Sst-Cre$^{+/-}$ and PV-Cre$^{+/-}$ mice were purchased from Jaxson Laboratory (Stock #: 006440, 013044 and 008069, respectively). All these strains were maintained on C57BL6/J background. We crossed Pten$^{fl/fl}$ mice with Sst-Cre$^{+/+}$ mice to generate Sst-Cre$^{+/-}$/Pten$^{fl/+}$ mice which were then backcrossed with Sst-Cre$^{+/+}$ mice to generate Sst-Cre$^{+/+}$/*Pten*$^{fl/+}$ breeders. By crossing the breeders we obtained three types of experimental mice, Sst-Cre$^{+/+}$/*Pten*$^{+/+}$ (Sst-Pten-WT), Sst-Cre$^{+/+}$/*Pten*$^{fl/+}$ (Sst-Pten-Het) and Sst-Cre$^{+/+}$/*Pten*$^{fl/fl}$ (Sst-Pten-KO) mice. They were all homozygous for Cre but expressed two, one or no copy of *Pten* in Sst neurons. Using the same

breeding strategy, we generated PV-Cre$^{+/+}$/Pten$^{fl/+}$ breeders and their offspring, PV-Cre$^{+/+}$/*Pten*$^{+/+}$ (PV-Pten-WT), PV -Cre$^{+/+}$/*Pten*$^{fl/+}$ (PV-Pten-Het) and PV-Cre$^{+/+}$/*Pten*$^{fl/fl}$ (PV-Pten-KO) mice. Both male and female littermates at the age of 4 - 8 weeks were used for behavioral assessments. Age and sex-matched C57BL/6 mice (purchased from Veterinary Resources at the University of Maryland School of Medicine) were used as social partners in modified three-chamber social tests. All mice were housed 2 - 5 per cage in ventilated racks in a temperature- and humidity-controlled animal room on a 12 h light/dark cycle with lights on from 07:00 to 19:00 and cared by the AAALAC accredited program of the University of Maryland School of Medicine. Autoclaved rodent chow and water were available *ad libitum*. The experimental protocol was approved by the Institutional Animal Care and Use Committees at the Hussman Institute for Autism and the University of Maryland School of Medicine.

4.2. Behavioral Assessments

Following procedures established in our previous work (Park et al., 2018), a series of behavioral assessments were conducted. Due to poor reproductive performance of mutant mice, multiple behavioral assessments were performed on the same groups of mice. Each mouse was tested for only one behavioral assessment per day. The behavioral tests were performed in the order of potential stress elicited from the tasks during the tests: open field test, elevated plus maze test, modified three-chamber social test, marble burying task, and rotarod test. Animals' activity during the behavioral assessments was recorded by a Logitech C920 HD Pro Webcam, with the Ethovision software (Noldus, RRID: SCR_002798) used for further offline analysis. All experiments were conducted during the light cycle with room lights at around 80 lux except for the elevated plus maze (around 8 lux). All areas were cleaned with 70% ethanol between test sessions, including areas untouched by mice.

4.2.1. Open field test

Mice were placed in the center of an open field apparatus (40 × 40 cm) and allowed to explore the field for 30 min. The movement was tracked using the Ethovision XT software. Distance moved and time spent in the center area (20 X 20 cm, square) and the corner area (15 X 15 cm, triangle) were further analyzed. Self-grooming behaviors were also analyzed from the open field activity using mouse behavior recognition (Detection settings for each mouse: posture between 70-90%, probability higher than 75%) in the Ethovision XT.

4.2.2. Elevated plus maze test

The elevated plus maze was composed of two open arms (30 × 5 cm) and two closed arms (30 × 5 cm) with wall height of 15 cm and 50 cm above the floor. Mice were individually placed in the center of the maze and facing one of the open arms. They were allowed to explore the open and closed arms of the maze for 10 min. The duration of time in arms was recorded. The percentage of time in open arms (or closed arms) was calculated as the duration in open arms (or closed arms) / total exploring duration.

4.2.3. Modified three-chamber social test

We used a modified apparatus to examine the social behaviors (Wu et al., 2020). The apparatus (40 (H) × 60 (L) × 20 (W) cm) was divided into three chambers (20 cm long for each chamber) made from white Plexiglass. The side chambers and the center chamber were separated by white Plexiglass walls with a small gate (10 cm) in the middle. Square interaction areas (10 × 10 cm) in each side chamber was formed by the gate and a three-sided fence made from clear Plexiglass (Figure 1A). Test mice entered these two areas to interact with social partners. The two side chambers were covered by a transparent Plexiglass sheet during the three-session test. In the first session (habituation), the test mouse was placed in the center chamber and allowed to

explore the chamber for 10 min. At the end of the habituation session, the test mouse was gently guided back to the middle of the center chamber, and the small gates were blocked. During the second session, which was to test the sociability, three novel C57BL/6 mice and three objects were placed in one of the two side chambers, respectively. The side chamber for social partners or objects was randomly assigned by flipping a coin. The test mouse was allowed to explore the center chamber for 10 min. After that, the test mouse was guided back to the middle of the center chamber again. In the third session, which was to test the social novelty preference, the objects were replaced by another set of three novel C57BL/6 mice, and the test mouse was allowed to explore the chamber for another 10 min. The duration that the animal spent in the interaction areas during each session was scored using the EthoVision XT software (Noldus). The preference index was calculated as duration exploring the novel mice / the total duration exploring the objects (or familiar mice) and the novel mice.

4.2.4. Marble burying task

Twelve glass marbles (3 × 4 arrangement) were placed on the surface of the bedding (5 cm deep) in standard mouse cages. The cages were covered with filter top lids during the test. Each test mouse was placed in the cage and allowed to explore for 30 min. The number of buried marbles was counted manually. The marble was checked from side of the cage. If the marble was buried more than 2/3 deep, it was counted as buried.

4.2.5. Rotarod test

The two-session rotarod test was conducted on an accelerating rotarod (Panlab, Harvard Apparatus) over two days. Mice were allowed to become acclimated to the stationary rod for 60s on the first day. Each test session consisted of three trials with 15-min inter-trial intervals (ITI). During each trial, mice were placed on the rotating rod (4 rpm) facing away from the direction of

rotation. The rotation speed was accelerated from 4 to 40 rpm over 5 min. If the mouse fell off the rod within 10 sec, the trial was repeated after 15 min, except for PV-Pten-KO mice, which had extreme difficulty staying on the stationary rod at all. The latency to fall was recorded as the time delay between the start of the trial and the moment when mice fell off the rod or made a complete revolution on the rod.

4.3. Statistical Analysis

Data were analyzed with SPSS (v.20) Software. All datasets were tested for normality using the Shapiro-Wilk test. For datasets with normal distribution, two-tailed Student's *t*-test (comparisons between two groups) or two-way ANOVA with repeated measured in one factor (rmANOVA) (comparisons among three groups) was used. Tukey's post hoc test was used for multiple comparisons after ANOVA test. For datasets with non-normal distribution, Kruskal-Wallis test with Dunn's post hoc test (comparison among three groups) was used. p-value < 0.05 was considered to be statistically significant.

CONFLICTS OF INTEREST

The authors declare no conflicts of interest.

AUTHOR CONTRIBUTIONS

Sangyep Shin: Investigation, Methodology, Formal analysis, Project administration, Visualization, Writing - original draft, Writing - review & editing. **Shiyong Huang**: Conceptualization, Methodology, Formal analysis, Project administration, Resources, Supervision, Visualization, Writing - review & editing.

ACKNOWLEDGEMENTS

We thank Dr. John Hussman, Dr. Gene Blatt, and Ms. Elizabeth Benevides for critical reading of the manuscript. We also thank Drs. Louis DeTolla and Turhan Coksaygan at the University of Maryland School of Medicine for providing veterinary and consulting services. This work was supported by Hussman Foundation grant HIAS18001 to S.H.

REFERENCES

Alcami, P., Marty, A., 2013. Estimating functional connectivity in an electrically coupled interneuron network. Proc Natl Acad Sci U S A. 110**,** E4798-807.

Ariza, J., et al., 2018. The Number of Chandelier and Basket Cells Are Differentially Decreased in Prefrontal Cortex in Autism. Cereb Cortex. 28**,** 411-420.

Asrican, B., et al., 2013. Next-generation transgenic mice for optogenetic analysis of neural circuits. Front Neural Circuits. 7**,** 160.

Association, A. P., 2013. Diagnostic and statistical manual of mental disorders: DSM-5. American Psychiatric Association, Washington, DC.

Baohan, A., et al., 2016. Pten and EphB4 regulate the establishment of perisomatic inhibition in mouse visual cortex. Nat Commun. 7**,** 12829.

Barker, K. T., Houlston, R. S., 2003. Overgrowth syndromes: is dysfunctional PI3-kinase signalling a unifying mechanism? Eur J Hum Genet. 11**,** 665-70.

Barnes, S. A., et al., 2015. Disruption of mGluR5 in parvalbumin-positive interneurons induces core features of neurodevelopmental disorders. Mol Psychiatry. 20**,** 1161-72.

Barrows, C. M., et al., 2017. PTEN Loss Increases the Connectivity of Fast Synaptic Motifs and Functional Connectivity in a Developing Hippocampal Network. J Neurosci. 37**,** 8595-8611.

Bridi, M. S., et al., 2017. Developmental Disruption of GABAAR-Meditated Inhibition in Cntnap2 KO Mice. eNeuro. 4**,** 1-14.

Buxbaum, J. D., et al., 2007. Mutation screening of the PTEN gene in patients with autism spectrum disorders and macrocephaly. Am J Med Genet B Neuropsychiatr Genet. 144B**,** 484-91.

Cao, W., et al., 2018. Gamma Oscillation Dysfunction in mPFC Leads to Social Deficits in Neuroligin 3 R451C Knockin Mice. Neuron. 97**,** 1253-1260 e7.

Carta, I., et al., 2019. Cerebellar modulation of the reward circuitry and social behavior. Science. 363.

Clipperton-Allen, A. E., Page, D. T., 2014. Pten haploinsufficient mice show broad brain overgrowth but selective impairments in autism-relevant behavioral tests. Hum Mol Genet. 23**,** 3490-505.

Clipperton-Allen, A. E., Page, D. T., 2015. Decreased aggression and increased repetitive behavior in Pten haploinsufficient mice. Genes Brain Behav. 14**,** 145-57.

Cupolillo, D., et al., 2016. Autistic-Like Traits and Cerebellar Dysfunction in Purkinje Cell PTEN Knock-Out Mice. Neuropsychopharmacology. 41**,** 1457-66.

Deng, X., et al., 2019. Parvalbumin interneuron in the ventral hippocampus functions as a discriminator in social memory. Proc Natl Acad Sci U S A. 116**,** 16583-16592.

Diaz-Ruiz, O., et al., 2009. Selective deletion of PTEN in dopamine neurons leads to trophic effects and adaptation of striatal medium spiny projecting neurons. PLoS One. 4**,** e7027.

Felix-Ortiz, A. C., Tye, K. M., 2014. Amygdala inputs to the ventral hippocampus bidirectionally modulate social behavior. J Neurosci. 34**,** 586-95.

Garcia-Junco-Clemente, P., et al., 2013. Overexpression of calcium-activated potassium channels underlies cortical dysfunction in a model of PTEN-associated autism. Proc Natl Acad Sci U S A. 110**,** 18297-302.

Goffin, A., et al., 2001. PTEN mutation in a family with Cowden syndrome and autism. Am J Med Genet. 105**,** 521-4.

Gregorian, C., et al., 2009. Pten deletion in adult neural stem/progenitor cells enhances constitutive neurogenesis. J Neurosci. 29**,** 1874-86.

Gunaydin, L. A., et al., 2014. Natural neural projection dynamics underlying social behavior. Cell. 157**,** 1535-51.

Hashemi, E., et al., 2017. The Number of Parvalbumin-Expressing Interneurons Is Decreased in the Prefrontal Cortex in Autism. Cereb Cortex. 27**,** 1931-1943.

Hitti, F. L., Siegelbaum, S. A., 2014. The hippocampal CA2 region is essential for social memory. Nature. 508**,** 88-92.

Hobert, J. A., et al., 2014. Biochemical screening and PTEN mutation analysis in individuals with autism spectrum disorders and macrocephaly. Eur J Hum Genet. 22**,** 273-6.

Hong, W., et al., 2014. Antagonistic control of social versus repetitive self-grooming behaviors by separable amygdala neuronal subsets. Cell. 158**,** 1348-1361.

Hussman, J. P., 2001. Suppressed GABAergic inhibition as a common factor in suspected etiologies of autism. J Autism Dev Disord. 31**,** 247-8.

Ito-Ishida, A., et al., 2015. Loss of MeCP2 in Parvalbumin-and Somatostatin-Expressing Neurons in Mice Leads to Distinct Rett Syndrome-like Phenotypes. Neuron. 88**,** 651-8.

Kayakabe, M., et al., 2013. Motor dysfunction in cerebellar Purkinje cell-specific vesicular GABA transporter knockout mice. Front Cell Neurosci. 7**,** 286.

Kwon, C. H., et al., 2006. Pten regulates neuronal arborization and social interaction in mice. Neuron. 50**,** 377-88.

Lauber, E., et al., 2018. Parvalbumin neurons as a hub in autism spectrum disorders. J Neurosci Res. 96**,** 360-361.

Lee, S., et al., 2018a. Shank2 Deletion in Parvalbumin Neurons Leads to Moderate Hyperactivity, Enhanced Self-Grooming and Suppressed Seizure Susceptibility in Mice. Front Mol Neurosci. 11**,** 209.

Lee, Y., et al., 2018b. Striatal Inhibition of MeCP2 or TSC1 Produces Sociability Deficits and Repetitive Behaviors. Exp Neurobiol. 27**,** 539-549.

Ljungberg, M. C., et al., 2009. Rapamycin suppresses seizures and neuronal hypertrophy in a mouse model of cortical dysplasia. Dis Model Mech. 2**,** 389-98.

Lugo, J. N., et al., 2014. Deletion of PTEN produces autism-like behavioral deficits and alterations in synaptic proteins. Front Mol Neurosci. 7**,** 27.

Maehama, T., Dixon, J. E., 1998. The tumor suppressor, PTEN/MMAC1, dephosphorylates the lipid second messenger, phosphatidylinositol 3,4,5-trisphosphate. J Biol Chem. 273**,** 13375-8.

Marin, O., 2012. Interneuron dysfunction in psychiatric disorders. Nat Rev Neurosci. 13**,** 107-20.

McBride, K. L., et al., 2010. Confirmation study of PTEN mutations among individuals with autism or developmental delays/mental retardation and macrocephaly. Autism Res. 3**,** 137-41.

Modi, M. E., Sahin, M., 2019. A unified circuit for social behavior. Neurobiol Learn Mem. 165**,** 106920.

Murray, A. J., et al., 2015. Parvalbumin-positive interneurons of the prefrontal cortex support working memory and cognitive flexibility. Sci Rep. 5**,** 16778.

Napoli, E., et al., 2012. Mitochondrial dysfunction in Pten haplo-insufficient mice with social deficits and repetitive behavior: interplay between Pten and p53. PLoS One. 7**,** e42504.

Okuyama, T., et al., 2016. Ventral CA1 neurons store social memory. Science. 353**,** 1536-1541.

Page, D. T., et al., 2009. Haploinsufficiency for Pten and Serotonin transporter cooperatively influences brain size and social behavior. Proc Natl Acad Sci U S A. 106**,** 1989-94.

Park, S. M., et al., 2018. Sex-Dependent Motor Deficit and Increased Anxiety-Like States in Mice Lacking Autism-Associated Gene Slit3. Front Behav Neurosci. 12**,** 261.

Perez, S. M., et al., 2019. Region specific knockdown of Parvalbumin or Somatostatin produces neuronal and behavioral deficits consistent with those observed in schizophrenia. Transl Psychiatry. 9**,** 264.

Peter, S., et al., 2016. Dysfunctional cerebellar Purkinje cells contribute to autism-like behaviour in Shank2-deficient mice. Nat Commun. 7**,** 12627.

Pfeffer, C. K., et al., 2013. Inhibition of inhibition in visual cortex: the logic of connections between molecularly distinct interneurons. Nat Neurosci. 16**,** 1068-76.

Rapanelli, M., et al., 2017a. The Role of Interneurons in Autism and Tourette Syndrome. Trends Neurosci. 40**,** 397-407.

Rapanelli, M., et al., 2017b. Targeted Interneuron Depletion in the Dorsal Striatum Produces Autism-like Behavioral Abnormalities in Male but Not Female Mice. Biol Psychiatry. 82**,** 194-203.

Reith, R. M., et al., 2013. Loss of Tsc2 in Purkinje cells is associated with autistic-like behavior in a mouse model of tuberous sclerosis complex. Neurobiol Dis. 51**,** 93-103.

Rudy, B., et al., 2011. Three groups of interneurons account for nearly 100% of neocortical GABAergic neurons. Dev Neurobiol. 71**,** 45-61.

Scheggia, D., et al., 2020. Somatostatin interneurons in the prefrontal cortex control affective state discrimination in mice. Nat Neurosci. 23**,** 47-60.

Selimbeyoglu, A., et al., 2017. Modulation of prefrontal cortex excitation/inhibition balance rescues social behavior in CNTNAP2-deficient mice. Sci Transl Med. 9.

Soghomonian, J. J., et al., 2017. Decreased parvalbumin mRNA levels in cerebellar Purkinje cells in autism. Autism Res. 10**,** 1787-1796.

Sohal, V. S., Rubenstein, J. L. R., 2019. Excitation-inhibition balance as a framework for investigating mechanisms in neuropsychiatric disorders. Mol Psychiatry. 24**,** 1248-1257.

Southwell, D. G., et al., 2020. Interneuron Transplantation Rescues Social Behavior Deficits without Restoring Wild-Type Physiology in a Mouse Model of Autism with Excessive Synaptic Inhibition. J Neurosci. 40**,** 2215-2227.

Stavarache, M. A., et al., 2015. The tumor suppressor PTEN regulates motor responses to striatal dopamine in normal and Parkinsonian animals. Neurobiol Dis. 82**,** 487-494.

Stiles, B., et al., 2004. PTENless means more. Dev Biol. 273**,** 175-84.

Stoodley, C. J., et al., 2017. Altered cerebellar connectivity in autism and cerebellar-mediated rescue of autism-related behaviors in mice. Nat Neurosci. 20**,** 1744-1751.

Sun, Q., et al., 2020. Ventral Hippocampal-Prefrontal Interaction Affects Social Behavior via Parvalbumin Positive Neurons in the Medial Prefrontal Cortex. iScience. 23**,** 100894.

Taniguchi, H., et al., 2011. A resource of Cre driver lines for genetic targeting of GABAergic neurons in cerebral cortex. Neuron. 71**,** 995-1013.

Tatsukawa, T., et al., 2018. Impairments in social novelty recognition and spatial memory in mice with conditional deletion of Scn1a in parvalbumin-expressing cells. Neurobiol Dis. 112**,** 24-34.

Tsai, P. T., 2016. Autism and cerebellar dysfunction: Evidence from animal models. Semin Fetal Neonatal Med. 21**,** 349-55.

Tsai, P. T., et al., 2012. Autistic-like behaviour and cerebellar dysfunction in Purkinje cell Tsc1 mutant mice. Nature. 488**,** 647-51.

Varga, E. A., et al., 2009. The prevalence of PTEN mutations in a clinical pediatric cohort with autism spectrum disorders, developmental delay, and macrocephaly. Genet Med. 11**,** 111-7.

Vogt, D., et al., 2015. The parvalbumin/somatostatin ratio is increased in Pten mutant mice and by human PTEN ASD alleles. Cell Rep. 11**,** 944-956.

Wang, W., et al., 2017. Striatopallidal dysfunction underlies repetitive behavior in Shank3-deficient model of autism. J Clin Invest. 127**,** 1978-1990.

Whitehouse, C. M., Lewis, M. H., 2015. Repetitive Behavior in Neurodevelopmental Disorders: Clinical and Translational Findings. Behav Anal. 38**,** 163-178.

Wu, N., et al., 2020. Identification of CDH11 as an ASD risk gene by matched-gene co-expression analysis and mouse behavioral studies. bioRxiv.

Zhang, B., Sudhof, T. C., 2016. Neuroligins Are Selectively Essential for NMDAR Signaling in Cerebellar Stellate Interneurons. J Neurosci. 36**,** 9070-83.

Zhang, L., et al., 2020. Hyperactivated PTP1B phosphatase in parvalbumin neurons alters anterior cingulate inhibitory circuits and induces autism-like behaviors. Nat Commun. 11**,** 1017.

Zikopoulos, B., Barbas, H., 2013. Altered neural connectivity in excitatory and inhibitory cortical circuits in autism. Front Hum Neurosci. 7**,** 609.

Zou, D., et al., 2016. DREADD in parvalbumin interneurons of the dentate gyrus modulates anxiety, social interaction and memory extinction. Curr Mol Med. 16**,** 91-102.